Synthesis and aggregation behavior of cyclic single- and double-tailed phosphate amphiphiles: A novel class of phosphate surfactants - Comparison with the aggregation behavior of sodium di-n-alkyl phosphates

Buwalda, Rixt; Wagenaar, Anno; Engberts, Jan B.F.N.

Published in:
European Journal of Organic Chemistry

DOI:
10.1002/jlac.199719970817

Synthesis and Aggregation Behavior of Cyclic Single- and Double-Tailed Phosphate Amphiphiles: A Novel Class of Phosphate Surfactants - Comparison with the Aggregation Behavior of Sodium Di-*n*-alkyl Phosphates

Rixt T. Buwalda, Anno Wagenaar, and Jan B. F. N. Engberts*

Department of Organic and Molecular Inorganic Chemistry, University of Groningen,
Nijenborgh 4, NL-9747 AG Groningen, The Netherlands
Fax: (internat.) +31(0)50/3634296
E-mail: J.B.F.N.Engberts@chem.rug.nl

Received February 21, 1997

Keywords: Cyclic phosphate amphiphiles / Micellization / Vesicle fusion / Bilayer packing / Vesicles / Amphiphiles

Herein we describe the synthesis and aggregation of the sodium salts of a series of 5-alkyl-2-hydroxy-1,3,2-dioxaphosphorinan-2-ones and 5,5-dialkyl-2-hydroxy-1,3,2-dioxaphosphorinan-2-ones in aqueous solution. The results are compared with properties of previously studied sodium di-*n*-alkyl phosphates. The single-tailed surfactants (**6a**, **b**, **g**) form micelles whereas the double-tailed ones (**6f**, **h**-**k**) form vesicles, as revealed by transmission electron microscopy (TEM). Critical micelle concentrations (CMC) for **6a**, **b**, **g** were determined using different techniques: UV spectroscopy, microcalorimetry, and conductometry. Phase transition temperatures of the bilayers were measured by differential scanning calorimetry (DSC) and by fluorescence depolarization. Fusion of the vesicles was studied employing the resonance energy transfer (RET) assay based on lipid mixing and TEM. Vesicles of **6h**-**k** fuse upon addition of Ca^{2+} or Mg^{2+} ions, to almost the same extent in each case. Fusion only takes place above the phase transition temperature (T_c) of the different bilayers. The threshold concentrations of Ca^{2+} and Mg^{2+} ions for fusion of the different vesicles are below 0.1 mM. The initial rate of fusion is high and precludes the measurement of accurate rate constants. Upon addition of calcium chloride different processes occur. Vesicle fusion, crystallization, and formation of multilamellar sheets were observed, as was apparent from experiments with vesicles formed from **6h**. Leakage through the vesicular bilayer of **6h** was determined by measuring the carboxyfluorescein release from the aqueous compartment of the vesicles. All data are consistent with the notion that the alkyl chain packing in the bilayers of the vesicles formed from the cyclic phosphates is less efficient than that in the bilayers of vesicles composed of di-*n*-alkyl phosphates.

Introduction

Surfactants are molecules with a dualistic character, consisting of a hydrophilic headgroup and a hydrophobic hydrocarbon chain. The characteristic feature of surfactants is their ability to form aggregates in aqueous solution. The morphology that these aggregates adopt, depends upon the molecular shape of the monomer, temperature, concentration, and added electrolytes[1]. Single-tailed surfactants usually form micelles whereas double-tailed surfactants often aggregate to form bilayers, the latter forming vesicles upon mechanical agitation.

Vesicles formed from synthetic bilayer-forming surfactants have been widely used as models for biological membranes[2-4]. Interestingly, biological and synthetic bilayers have many properties in common such as phase transitions and fusion behavior. Properties of biological cells often can be successfully mimicked by using vesicles formed from synthetic amphiphiles. Fusion is usually induced by a fusogenic agent and is a two-step process. In the first step, which involves aggregation, vesicles cluster as a result of dehydration of the headgroups and a reduction of repulsive electrostatic forces. In the second step the actual fusion process takes place. Due to local defects in the bilayer, vesicles conglomerate with mixing of their aqueous contents. Below the phase transition temperature (T_c) bilayers are in the gel state, in which lateral diffusion is slow and the hydrocarbon chains are in an *all-trans* conformation. Above T_c, bilayers are in the liquid-crystalline state, *gauche* conformations occur and lateral diffusion is fast. For efficient fusion, bilayers should be in the liquid-crystalline state.

Surfactants with a heterocyclic ring near the headgroup[5] especially those possessing an 1,3-dioxane and 1,3-dioxolane ring have become of great interest in the past decade as a result of their chemodegradability. Although properties as CMC and Krafft points have been investigated, neither the phase behavior of the bilayers nor the fusogenic properties have been assessed in detail.

Properties of sodium di-*n*-alkyl phosphate vesicles have been described in previous studies[6]. Symmetric and asymmetric sodium di-*n*-alkyl phosphates have been investigated with regard to their fusogenic and polymorphic behavior[6a]. In another study the effect of counterion binding on the phase transition temperature of di-*n*-alkyl phosphate vesicles was investigated[6f]. The purpose of the present work was to investigate the properties of micelles and vesicles formed from the sodium salts of a series of 5-alkyl-2-hydroxy-1,3,2-dioxaphosphorinan-2-ones and from the sodium salts of several 5,5-dialkyl-2-hydroxy-1,3,2-dioxaphos-

  0947-3440/97/0808-1745 $ 17.50+.50/0

phorinan-2-ones, respectively. It was anticipated that the change in headgroup structure would influence the bilayer packing and therefore the vesicles might show modified aggregation and phase behavior. This was borne out in practice.

Scheme 1. Molecular structures of compounds **6**

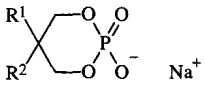

a: $R^1 = C_{10}H_{21}$, $R^2 = H$; **i:** $R^1 = C_{12}H_{25}$, $R^2 = C_{16}H_{33}$
b: $R^1 = C_{12}H_{25}$, $R^2 = H$; **j:** $R^1 = C_{14}H_{29}$, $R^2 = C_{14}H_{29}$
f: $R^1 = C_{10}H_{21}$, $R^2 = C_{10}H_{21}$; **k:** $R^1 = C_{16}H_{33}$, $R^2 = C_{16}H_{33}$
g: $R^1 = C_{12}H_{25}$, $R^2 = CH_3$ **l:** $R^1 = C_{18}H_{35}$, $R^2 = C_{18}H_{35}$
h: $R^1 = C_{12}H_{25}$, $R^2 = C_{12}H_{25}$

Results and Discussion

As expected[1], all single-tailed surfactants (**6a**, **b**, and **g**) investigated in this study, form micelles. Critical micelle concentrations were determined using microcalorimetry, UV spectroscopy, and conductometry. The double-tailed phosphorinanes **6h**, **i**, **j**, and **k** form vesicles as revealed by transmission electron microscopy. Fusion of the vesicles with Ca^{2+} and Mg^{2+} ions as the fusogenic agent was investigated using the RET assay and TEM.

CMC Measurements

Critical micelle concentrations of **6a**, **b**, and **g** are listed in Table 1. The trend in the CMC values is as anticipated: the CMC decreases upon increasing chain length and decreases upon increasing chain branching[2]. The critical micelle concentration of **6b** is higher than that of **6g**. If the additional methyl moiety in **6g** is viewed as a branch, the decrease in CMC of **6g** relative to that of **6b** is in line with expectation. Critical micelle concentrations of the sodium alkylhydroxy phosphates[7] with corresponding alkyl chain lengths are lower than those of **6a**, **b** and **6g** with corresponding alkyl chain lengths. Since the CMC is a measure of the thermodynamic stability of a micelle, micelles formed from phosphorinanes are more stable than sodium alkylhydroxy phosphate micelles. In fact, the hydrophobic moieties of the phosphorinanes are larger than those of sodium alkylhydroxy phosphates with a comparable number of carbon atoms in the hydrocarbon chain, which is a result of the additional methylene groups in the six-membered ring connected to the head group of the former. Thus, despite the change in headgroup structure of the phosphorinanes relative to the sodium alkylhydroxy phosphates, methylene groups in the six-membered ring of the phosphorinanes, appear to contribute to the hydrophobicity of the surfactant molecule.

Critical micelle concentrations for **6b** and **6g** were determined by three and two different methods, respectively (Table 1). As shown in Table 1, all three methods give comparable results. The presence of pinacyanol chloride as a reporter molecule does not significantly affect the CMC.

Table 1. Critical micelle concentrations (mM) for single-tailed phosphorinanes

Compound	Conductometry	Microcalorimetry	Pinacyanol
6a			11.08
6b	2.84	2.6	2.66
6g		1.9	1.96

Electron Microscopy

Transmission electron microscopy experiments were carried out using uranyl acetate (UAc) as a stain and coloring material. The results showed that the phosphorinanes **6h-k** form unilamellar vesicles varying in size from 25-90 nm. In the case of **6l**, no vesicles were observed with TEM. Therefore, other experiments were performed to elucidate the aggregation behavior of **6l** in water (see fluorescence depolarization and I_1/I_3 measurements). By means of cryo electron microscopy, a diameter ranging from 30 to 70 nm was observed for vesicles formed from **6h**.

For the different vesicular systems addition of Ca^{2+} or Mg^{2+} ions not only induced fusion, but crystal formation was observed as well. Crystallization started immediately after the addition of Ca^{2+} or Mg^{2+} ions. Apparently, fusion is accompanied by crystallization. Both unilamellar and multilamellar fused vesicles, ranging in size from 150 to 1000 nm, were observed by TEM. After the addition of EDTA, smaller vesicles were formed, even though the crystals did not completely disappear. Figures 1a-e show a series of electron micrographs of vesicles formed from **6h**.

In the case of sodium di-*n*-alkyl phosphate vesicles, addition of Ca^{2+} leads to fusion followed by the formation of tubular structures (after about 5 minutes), which turned out to be anhydrous calcium di-*n*-alkyl phosphate crystals[8]. In the present vesicular systems, fusion and crystallization took place immediately after the addition of fusogenic agent and no tubular structures were observed. Apparently, the phosphorinanes are unable to form a highly ordered three-dimensional array with Ca^{2+} ions akin to that found in the tubes formed from calcium di-*n*-alkyl phosphates. This is probably due to the fact that the phosphorinane headgroup is too bulky (due to the six-membered ring connected to the phosphate headgroup), thus preventing effective packing in a highly ordered way.

A vesicle solution of **6h** was studied using cryo electron microscopy. In a typical experiment Ca^{2+} ions (0.05 mM) were added to a vesicle solution of **6h**, leading to immediate vitrification of the sample. Using the negative staining method, both fusion and crystallization were observed. Vesicles varied in size from 50 to 160 nm, indicating that both fused and unfused vesicles were present. In addition to observations from the negative staining method, multilamellar sheets were observed by cryo TEM. The distance between the lamellar layers was found to be 44 Å, which is typical for a bilayer distance.

Figure 1. Electron micrographs of (A) vesicles formed from **6h**, (B) after addition of Ca^{2+} (0.05 mM), (C) vesicles formed after addition of EDTA, (D) vesicles of **6h** upon addition of Mg^{2+} (0.05 mM) and (E) vesicles obtained after addition of EDTA; the bar represents 200 nm

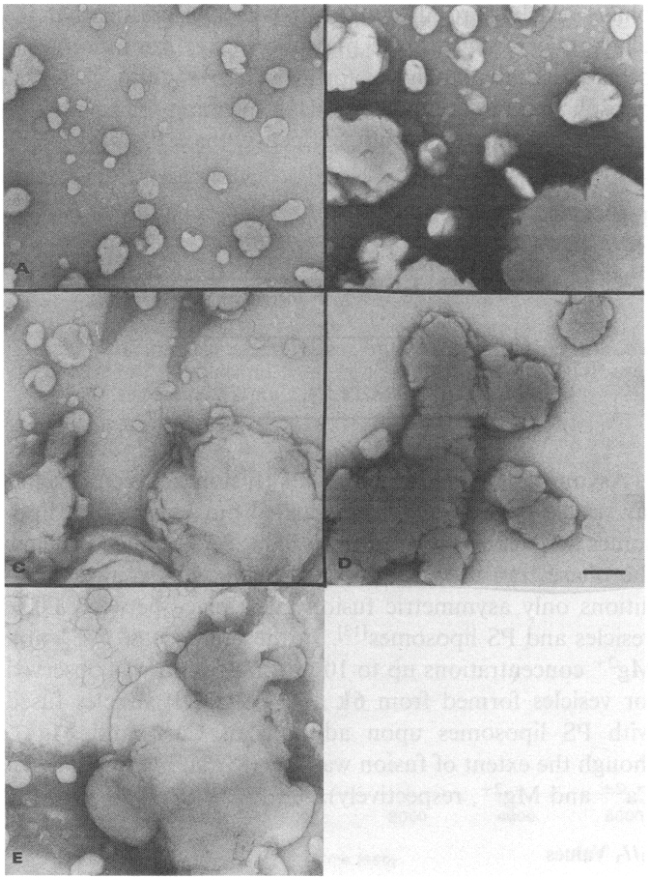

Differential Scanning Microcalorimetry

Phase transition temperatures, T_c, of **6h-k** are summarized in Table 2. For **6h**, no transition was found in the temperature range from 5 to 90°C. The trend in phase transition temperatures reflects the packing efficiency in the vesicular bilayers. As expected, T_c increases with increasing length of the alkyl chains, R^1 and R^2[9]. For comparison, phase transition temperatures of sodium di-*n*-alkyl phosphate vesicles[9,10] with corresponding alkyl chain lengths are also given in Table 2. Clearly, the T_c values for the bilayers formed from phosphorinanes are lower than those for bilayers of sodium di-*n*-alkyl phosphates of corresponding alkyl chain length. This indicates that the bilayer of the phosphorinanes is less stable, owing to a less efficient bilayer packing relative to bilayers of di-*n*-alkyl phosphates. Inspection of molecular models shows that the headgroup of the phosphorinanes is bulkier than that of sodium di-*n*-alkyl phosphates due to the six-membered ring connected to the former. This results in a decrease in the efficiency of alkyl chain packing of the phosphorinanes compared to that for di-*n*-alkyl phosphates.

The enthalpograms recorded for vesicles formed from **6i** and **6j** showed several small peaks in addition to a main peak which was attributable to the main phase transition. Apparently, the main phase transition for bilayers of **6i** and **6j** (at 24 at 32°C, respectively) is accompanied by small pretransitions. In the enthalpogram of vesicles formed from compound **6k** only one sharp peak was observed at 51°C.

Table 2. Phase transition temperatures determined by DSC

Compound R^1, R^2	T_c (°C)	
	phosphorinanes	di-*n*-alkyl phosphates
$C_{12}H_{25}$, $C_{12}H_{25}$	8[a]	35
$C_{14}H_{29}$, $C_{14}H_{29}$	32	52
$C_{16}H_{33}$, $C_{16}H_{33}$	51	66
$C_{12}H_{25}$, $C_{16}H_{33}$	24	39[a]

[a] Determined by fluorescence depolarization.

Fluorescence Depolarization

This is a standard technique for studying the physical state of a bilayer[11,12]. DPH (*trans,trans,trans*-1,6-diphenylhexa-1,3,5-triene) intercalated in the core of the bilayer reports physical changes in the hydrophobic interior of the bilayer. For vesicles formed from compounds **6i** and **6j** no cooperative transition was observed using fluorescence depolarization. For vesicles formed from **6h** and **6k** cooperative transitions were observed at 8 and 52°C, respectively. The phase transition temperature for **6k** as determined by DSC is in reasonable agreement with the value obtained by fluorescence depolarization. The slightly earlier apparent onset of melting in the fluorescence depolarization experiment may be a consequence of the presence of the probe within the bilayer leading to the earlier onset of melting. It is striking that the transitions of **6i** and **6j** are noncooperative whereas **6h** and **6k** show cooperative transitions. For vesicles formed from the sodium di-*n*-alkyl phosphates all phase transitions are cooperative[9], which is consistent with the notion that the packing of those bilayers is more efficient than that of bilayers formed from the sodium salts of 5,5-dialkyl-2-hydroxy-1,3,2-dioxaphosphorinan-2-ones.

Fusion Experiments

Vesicle fusion was monitored using the RET assay at a temperature above T_c. Fusion experiments for vesicles formed from **6h**, **i**, **j**, and **k** were performed at 22, 40, 48, and 65 °C, respectively. Ca^{2+} and Mg^{2+} ions were employed as fusogenic agents. Since a change in fluorescence intensity may also result from a reversible transition in the bilayer induced by the fusogenic agent, the final extent of fusion was measured after addition of an excess of EDTA, a binding agent for Ca^{2+} and Mg^{2+}. Below T_c, no fluorescence increase was observed for vesicles prepared from **6k**. The observation that lipid mixing only takes place with membranes in the liquid crystalline state is in agreement with previous results[6].

The extent of fusion as a function of Ca^{2+} and Mg^{2+} concentrations is plotted in Figures 2a and 2b, respectively. It is striking that the extent of fusion induced by Ca^{2+} and Mg^{2+} is similar. The maximum extents of fusion are listed in Table 3.

For vesicles formed from the sodium di-*n*-alkyl phosphates no Mg^{2+} -induced fusion was observed[6c], although massive aggregation took place. It was also shown that Mg^{2+} ions inhibit Ca^{2+}-induced fusion of DDP vesicles. This was ascribed to the fact that Mg^{2+} displays a higher binding constant for DDP than Ca^{2+}. Presumably, Mg^{2+} cannot form a dehydrated *trans* complex between two adjacent DDP vesicles, which is a prerequisite of fusion. Since Mg^{2+} ions do induce fusion of phosphorinane vesicles, it would seem that Mg^{2+} is able to form a *trans* complex between vesicles formed from phosphorinane amphiphiles. For **6k**, variable and rather irreproducible fusion results were observed which were not studied further.

Figure 2. (a) Extents of fusion as a function of the Ca^{2+} concentration for **6h** (triangles), **6i** (circles) and **6j** (squares) at 22, 40, and 48°C, respectively; (b) extents of fusion as a function of the Mg^{2+} concentration for **6h**, **6i**, and **6j** at the temperatures given above; lipid concentrations was 50 μM

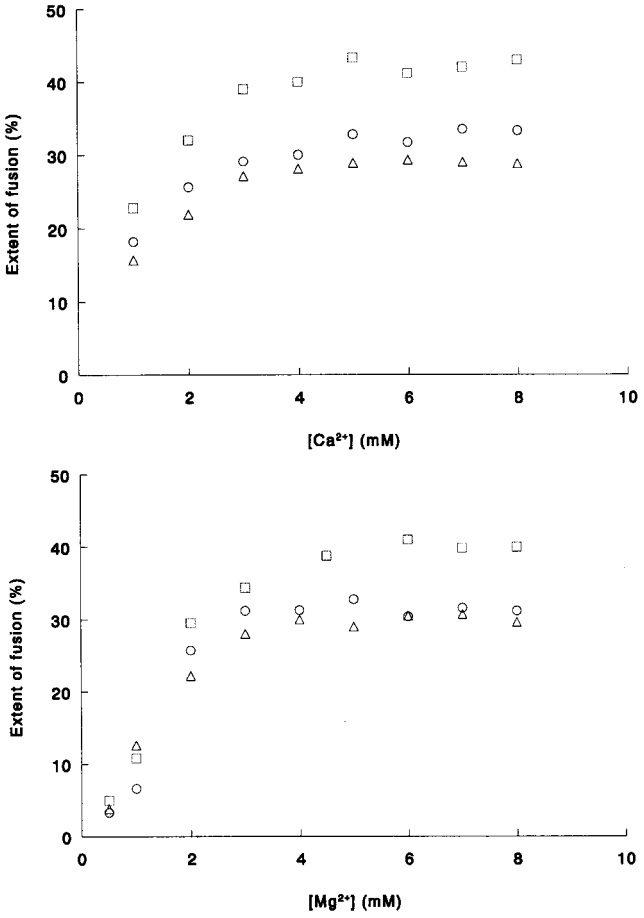

Initial rates of fusion were too fast to be measured accurately. Rates in the order of 20 to 80% s^{-1} were observed. Sodium di-*n*-alkyl phosphate vesicles show lower initial rates of fusion, for example for DDP[6c]: 4.5% s^{-1} (9 mM of Ca^{2+} at 40°C). Furthermore, threshold concentrations of Ca^{2+} and Mg^{2+} ions for fusion are low for vesicles formed from the phosphorinanes (below 0.1 mM). Threshold concentrations found for di-*n*-alkyl phosphate vesicles are considerably higher, for example 1.7 mM Ca^{2+} for DDP vesicles.

The observations that the dioxaphosphorinane vesicles fuse in the presence of Mg^{2+} as well as of Ca^{2+}, possess lower threshold concentrations for fusion and higher initial rates of fusion as compared to the sodium di-*n*-alkyl phosphate vesicles, are all consistent with the notion that the bilayers formed from the phosphorinanes are more easily destabilized than bilayers formed from sodium di-*n*-alkyl phosphates. Apparently, the bilayer packing for sodium di-*n*-alkyl phosphates is more effective than that for phosphorinane surfactants.

Table 3. Maximum extents of fusion of vesicles formed from **6h**, **6i** and **6j**

Compound	Fusogenic agent	
	Ca^{2+}	Mg^{2+}
6h	29	30
6i	33	32
6j	43	41

Asymmetric fusion experiments (fusion between dissimilar vesicle populations) were carried out between PS liposomes and vesicles formed from **6k** at 25°C, which is below the phase transition temperature of **6k**. Under these conditions only asymmetric fusion takes place between DDP vesicles and PS liposomes[13]. In the presence of Ca^{2+} and Mg^{2+} concentrations up to 10 mM, no fusion was observed for vesicles formed from **6k** and PS. DDP vesicles fused with PS liposomes upon addition of Ca^{2+} and Mg^{2+}, though the extent of fusion was low (8% and 4% with 8 mM Ca^{2+} and Mg^{2+}, respectively).

I_1/I_3 Values

The intensity ratio between the first and the third peak in the fluorescence spectrum of pyrene, the I_1/I_3 value, gives a measure of the environment at the pyrene binding sites[14]. A mean I_1/I_3 value of 1.13 was found for aggregates formed from **6l**, indicative of an "aromatic solvent environment" for pyrene. Since a lower I_1/I_3 value was expected, it is not clear what kind of aggregates are formed by **6l** in aqueous solution.

X-ray Diffraction

Low-angle X-ray diffraction patterns were obtained from vesicle solutions of **6h** to which Ca^{2+} and Mg^{2+} ions (both 0.5 mM) had been added. After irradiation, a ring pattern was observed, which did not resemble the X-ray pattern produced by suspensions of synthetically prepared Ca^{2+} and Mg^{2+} salts of **5h**.

A wide-angle X-ray diffraction pattern was obtained from a vesicle solution of **6h** to which Ca^{2+} (0.5 mM) had been added. The resulting pattern showed one ring corresponding to a lattice distance of 43 Å. This result was corroborated by cryo electron microscopy; the cryo electron micrographs revealed multilamellar layers with a separation of 43 Å. Again, these results contrast with those obtained following the addition of Ca^{2+} to NaDDP vesicles. In the latter case, tubular structures were formed, which were identified as calcium di-*n*-alkyl phosphate crystals[8].

Encapsulation Experiments

Leakage of carboxyfluorescein from vesicles formed from **6h** and cholesterol (80/20) and DDP and cholesterol (80/20) was determined by monitoring the carboxy fluorescein release from the vesicles as a function of time.

Leakage from vesicles prepared from **6h** and cholesterol (80/20) was found to be faster than that from vesicles formed from DDP and cholesterol (80/20), Figure 3. Though the leakage rates showed some variations between experiments, the above statement held true throughout. This observation is again consistent with the notion that bilayers of vesicles of bilayer-forming phosphorinanes are less efficiently packed than those in di-*n*-alkyl phosphate vesicles.

Figure 3. Carboxyfluorescein release from vesicles formed from **6h** and cholesterol (80/20) and from vesicles formed from DDP and cholesterol (80/20) in a HEPES buffer at pH = 7.4

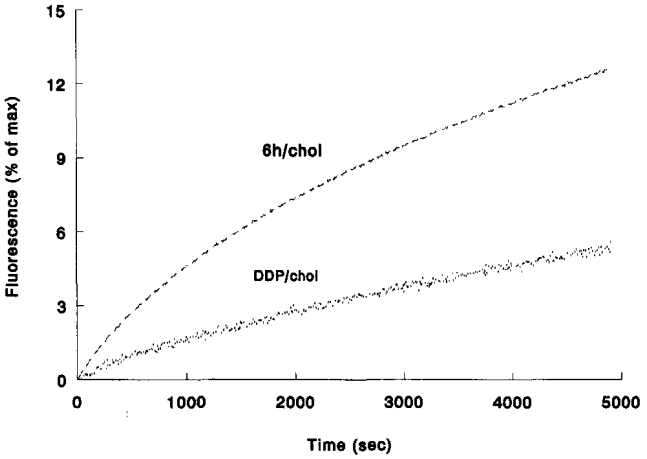

Conclusions

The present study shows that the novel single-tailed surfactants (**6a**, **b**, and **g**) form micelles and the double-tailed ones (**6h**, **i**, **j**, **k**) vesicles, with the exception of **6l**. Critical micelle concentrations decrease with increasing chain length and decrease with increasing branching. Critical micelle concentrations for the single-tailed phosphorinanes are lower than those of sodium alkylhydroxy phosphates. Vesicles of **6h**, **i**, and **j** fuse with Ca^{2+} as well as with Mg^{2+} ions as revealed by lipid mixing assays and by electron microscopy. Properties of vesicles formed from bilayer-forming phosphorinanes differ in various respects from those of sodium di-*n*-alkyl phosphate vesicles studied previously. Phase transition temperatures of vesicles formed from bilayer-forming phosphorinanes are lower than those of vesicles of sodium di-*n*-alkyl phosphates and initial rates of lipid mixing are higher. Furthermore, vesicles prepared from **6h** and cholesterol are more susceptible to leakage than those formed from DDP and cholesterol. All observations are consistent with the notion that the packing of alkyl chains in the bilayer of vesicles formed from the newly synthesized bilayer-forming phosphorinanes is less efficient than that in vesicles formed from sodium di-*n*-alkyl phosphates. The variation in headgroup structure of bilayer-forming phosphate surfactants leads to a difference in bilayer packing which markedly influences the properties of the bilayer.

We gratefully acknowledge *J. F. L. van Breemen* for performing the electron and cryo electron microscopic measurements, Drs. *W. Meyberg* for the DSC measurements and Dr. *M. ter Beest* for his help with the encapsulation experiments.

Experimental Section

Materials: Melting points were determined on a Kofler hot-stage and are uncorrected. - ^{1}H-NMR, ^{13}C-NMR and ^{31}P-NMR spectra were measured at 200 or 300 MHz on a Varian Gemini-200 or a Varian VXR-300 spectrometer, respectively, using solutions in $CDCl_3$ unless otherwise stated. The chemical shifts are reported in δ units (ppm) relative to the protonated solvent as an internal standard and converted to the TMS scale (δ = 0.00). - Petroleum ether showed a boiling range of 40-60°C, unless otherwise stated.

N-[(7-Nitrobenz-2-oxa-1,3-diazol-4-yl)phosphatidyl]ethanolamine (*N*-NBD-PE), *N*-[(lissamine rhodamine-B-sulfonyl)phosphatidyl]ethanolamine (*N*-Rh-PE) and phosphatidyl serine (PS, from bovine brain) were obtained from Avanti Polar Lipids, Inc. 4-(2-Hydroxyethyl)piperazine ethanesulfonic acid (HEPES) was purchased form Sigma Chemical Co.; sodium acetate, ethylenediamine tetraacetic acid (EDTA), and calcium and magnesium chlorides were obtained from Merck. Pinacyanol was purchased from Acros Chimica. 5(6)-Carboxyfluorescein (CF) was purchased from Eastman Kodak Co. and was purified as described elsewhere[15]. Triton X-100 was obtained from BDH Chemicals Ltd. Water was twice distilled in an all-quartz apparatus.

CMC Measurements: Critical micelle concentrations were determined by conductivity measurements. Conductivities were measured using a Wayne-Kerr Autobalance Universal bridge B642 fitted with a Philips electrode PW 9512101 with a cell constant of 0.71 cm^{-1}. The conductivity cell was equipped with a magnetic stirrer. CMC values were derived from the intersections of the tangents drawn before and after the discontinuity in the conductivity versus concentration plot.

Critical micelle concentrations were also determined by titration microcalorimetry[16]. Enthalpograms were recorded using a Microcal Omega titration microcalorimeter (Microcal Northampton, MA, USA). The solutions were degassed prior to use. In a typical experiment the sample and reference cell were filled with water, while a syringe was filled with the surfactant solution at a concentration of approximately 20 times the CMC. The contents of the sample cell were stirred. After thermal equilibrium had been reached, the first aliquot was injected and the heat absorbed or evolved was recorded. Once thermal equilibrium had been attained, the next aliquot was injected. This procedure was repeated until the desired concentration range had been covered. Raw data were analyzed using Omega software (Origin 2.9).

UV measurements were performed using pinacyanol chloride[17]. Pinacyanol chloride (10^{-5} M) was added to surfactant solutions of several concentrations, ranging from below to above the (estimated) CMC. Below the CMC, the absorption spectrum of pinacyanol chloride resembles that of the dye in polar media. The absorption spectrum changes sharply at the CMC and resembles that of pinacyanol chloride in organic solvents.

Vesicle Preparation: The different vesicles were prepared by sonicating a known amount of lipid in aqueous solution above T_c with a Branson B15 sonifier cell disruptor for 4 minutes. Since the sonication method failed for **6l**, the ethanol injection method[18] was used instead. For this 4 mg of **6l** was dissolved in 100 µl of ethanol.

Using a preheated Hamilton micro syringe, 80 µl of this solution was injected into 1 ml of water at 55 °C with stirring.

Vesicles labeled with fluorescent probes were prepared by dissolving the lipids in Rh and NBD solutions. The solvent was evaporated under an N_2 stream and the film was further dried in vacuo. After addition of 1 ml of water and sonication for 4 min, the vesicle solution was obtained. A labeled vesicle solution of phosphatidyl serine was sonicated for 1 minute.

Differential Scanning Microcalorimetry (DSC): Differential isobaric heat capacities as a function of temperature were recorded for water and the different vesicles prepared from **6h** to **6k** using an MLS differential scanning microcalorimeter from Microcal. Scans were recorded from 5 to 90°C. Rescans were performed to check the reversibility of the transition. The main phase transition (between the liquid crystalline and the gel phase) is accompanied by a peak in the trace. Since in previous microcalorimetric studies[19] it had been shown that the presence of ethanol may influence the main phase transition, vesicles were prepared by sonication instead of the ethanol injection method.

Fluorescence Depolarization[11]: Phase transition temperatures (T_c) were measured using the rod-like fluorescent probe *trans, trans,trans*-1,6-diphenylhexa-1,3,5-triene (DPH) intercalated in the hydrophobic core of the bilayer. Polarized light is absorbed by the DPH molecules and subsequently emitted. The polarization *P* characteristic of the differences between emitted and absorbed light, is given by Equation 1.

$$P = \frac{I_{\parallel} - I_{\perp}}{I_{\parallel} + I_{\perp}} \qquad (1)$$

In this equation, $I_{\parallel}$ and $I_{\perp}$ denote the intensities of light polarized parallel and perpendicular to the absorbed light, respectively. Vesicle bilayers in the gel state typically show *P* values in the range of 0.3-0.4 whereas *P* values ranging from 0.02-0.1 are observed for bilayers in the liquid-crystalline state. Measurements were performed as described previously[9]. At each temperature the solution was equilibrated for at least 15 minutes, the polarization was measured and calibrated three times. The amphiphile concentration was $5 \cdot 10^{5}$ M.

Fusion Experiments: Vesicle fusion was monitored using a resonance energy transfer (RET) assay[20] based on lipid mixing. Vesicles labelled with 0.8 mol-% each of *N*-NBD-PE and *N*-Rh-PE were mixed with an equimolar amount of unlabeled vesicles. In fusion experiments the lipid concentration was 50 µM. Fusion was induced by adding a fusogenic agent (Ca^{2+} or Mg^{2+} ions). Upon bilayer mixing dilution of the fluorophores takes place, the transfer efficiency decreases and an increase in NBD fluorescence is observed. The decrease in transfer efficiency was continuously monitored on an SLM-Aminco SPF-500C spectrofluorometer equipped with a thermostatted cell holder, a magnetic stirring device and a chart recorder. The excitation wavelength was 475 nm, the emission wavelength 530 nm.

The fluorescence scale was calibrated by setting the initial fluorescence of the labeled and non-labeled vesicles equal to 0%. The fluorescence value at infinite dilution (100% fluorescence) was determined after each experiment by adding Triton X-100 (final concentration 1%, v/v). Corrections were made for sample dilution and the effect of the surfactants on the quantum yield of NBD. The extent of fusion was determined after addition of an excess of EDTA (based on Ca^{2+} or Mg^{2+}), a Ca^{2+} and Mg^{2+} binding agent.

In asymmetric fusion experiments phosphatidyl serine (PS) vesicles were labeled with 0.8 mol-% each of *N*-NBD-PE and *N*-Rh-PE.

Electron Microscopy: Transmission electron micrographs were obtained using a Philips EM 300, EM 201, or JEM 1200 EX electron microscope operating at 80 kV. Samples were prepared on carbon-coated Formvar grids, pretreated by glow discharge in *n*-pentylamine. Samples were stained with 1% or 0.1% (w/v) uranyl acetate[21]. Cryo electron microscopy was performed using a JEM 1200 EX or a Philips CM 20 microscope. Vesicles of **6h-k** were examined before and after addition of Ca^{2+} and Mg^{2+} by the negative staining method. EDTA was added in an 8-fold excess. Vesicles of **6h** were examined by cryo electron microscopy before and after addition of Ca^{2+}. In a typical experiment 3 µl of a 0.1 M $CaCl_2$ solution was mixed with 40 µl of a 5.4 mM vesicle solution of **6h**. The suspension was immediately vitrified (time between mixing and vitrification was about 20 seconds) in liquid ethane.

X-ray Diffraction: Vesicle solutions of **6h** were prepared by sonication. The amounts of **6h** and $CaCl_2$ used, were similar to those employed in the cryo EM experiment. The concentration of Mg^{2+} was equal to that of Ca^{2+}. Synthetic Ca^{2+} and Mg^{2+} salts of **5h** were prepared as described previously[6].

Suspensions of the crystals in water were transferred into a capillary which was sealed with wax. Diffraction patterns were taken with a precession camera at a wavelength of 1.5418 nm (the Cu-K_α line).

I_1/I_3 Values: The fluorescence spectrum of pyrene[14] shows five vibrational peaks (1 to 5) in the range 365 to 400 nm. The intensity of the third peak relative to the first one is dependent on the medium in which pyrene is dissolved. Therefore, the ratio of peak 1 (372-373 nm) to peak 3 (383 nm), I_1/I_3, is taken as a measure of the polarity of the binding site at which pyrene is located. In polar media, the ratio I_1/I_3 ranges from 1.25-2.00, in aromatic solvents from 1.00-1.25 and in hydrocarbon solvents from 0.55-0.65. Pyrene incorporated in bilayers shows an I_1/I_3 value close to that for apolar media.

Aggregates of **6l** were made by the ethanol injection method as described previously[17]. Pyrene was dissolved in the ethanol at such a concentration that in the final solution a pyrene concentration of 10^{-7} M was acchieved.

Spectra were recorded on an SLM-Amino SPF-500C spectrofluorometer. The excitation wavelength was 335 nm, spectra were recorded over the range 365 to 395 nm in steps of 0.25 nm. The bandpass was 5 nm.

Encapsulation Experiments: Vesicle solutions of **6h** in combination with cholesterol were prepared in a 20 mM carboxyfluorescein (CF) solution by sonication. The non-encapsulated material was removed on a Sephadex G-75 column at room temperature with an elution buffer (150 mM NaCl, 5 mM NaOAc, 5 mM HEPES at pH = 7.4). CF was encapsulated at self-quenching concentrations. Release of CF to the extravesicular medium results in an increase of the CF fluorescence which is proportional to the amount of leakage[22]. CF leakage was monitored using an SLM-Aminco SPF-500 spectrophotometer equipped with a thermostatted cell holder and a magnetic stirring device. The excitation wavelength was 430 nm, the emission wavelength 513 nm. The initial fluorescence value was taken as 0% leakage, the level of 100% fluorescence was obtained after addition of Triton X-100 (final concentration 1%, v/v). Corrections were made for sample dilution.

The lipid concentration was between 1.4 mM for DDP/Chol and 2.0 mM for **6h**/Chol.

Syntheses (see Scheme 2)

Diethyl 2-Alkylmalonates: All compounds have been described in the literature: **1a**[23], **1b**[23], **1c**[24], **1d**[23], **1e**[25].

Diethyl 2-(cis-9-Octadecenyl)malonate[25] (**1e**): To a solution of 0.851 g (0.037 mol) of sodium in 75 ml of absolute ethanol, 5.6 g (0.035 mol) of diethyl malonate was added dropwise at 70°C. After stirring for 30 minutes at 70°C, 14.0 g (0.037 mol) of *cis*-9-octadecenyl iodide was added over a period of 10 min. The reaction mixture was then refluxed for 1 h. After cooling the ethanol was evaporated under reduced pressure. The yellow-brown slurry was dissolved in 100 ml of diethyl ether, washed with 35 ml of water and 25 ml of a saturated NaCl solution. The organic phase was dried with Na_2SO_4, filtered and the solvent was removed under reduced pressure. The viscous oil (14.6 g) was purified by column chromatography on 200 g of silica gel, using hexane/CH_2Cl_2 (1:1) as the eluent. Yield: 7.1 g (50%) of **1e**. - ^{1}H NMR: δ = 0.86 (t, 3H, CH_3), 1.24 (m, 30H, CH_2), 1.86 (m, 2H, CH_2), 1.97 (m, 4H, CH_2), 3.28 (t, 1H, CH), 4.17 (q, 4H, CH_2), 5.32 (m, 2H, CH=CH). - ^{13}C NMR: δ = 169.43 (C=O), 129.8 (CH=CH), 61.1 (CH_2O), 52.0 (CH), 32.5, 31.8, 29.7, 29.6, 29.4, 29.3, 29.2, 29.1, 28.7, 27.2, 27.1, 22.6 (CH_2, alkyl chain), 14.0 (CH_3).

Diethyl 2,2-Dialkylmalonates (**2f-l**): The second alkylation was performed in the same way as the mono alkylation. The compounds **2f-k** have been described in the literature: **2f**[26], **2g**[24], **2h**[27], **2i**[28], **2j**[29], **2k**[30].

Diethyl 2,2-Bis(cis-9-Octadecenyl)malonate (**2l**): Sodium hydride (0.35 g, 0.01 mol) was washed with hexane before 5 ml of DMF was added. A solution of 4.1 g (0.01 mol) of **1e** in 10 ml of DMF was added dropwise. The reaction mixture was stirred for 1 h. A solution of 3.79 g (0.01 mol) *cis*-9-octadecenyl iodide in 10 ml of hexane was then added, and the mixture was heated for 8 h at 80°C. After cooling, the mixture was poured into 200 ml of diethyl ether and 50 ml of water. Separation was difficult and took several hours, hence some NaCl was added. The organic layer was dried with Na_2SO_4 and the solvent was removed under reduced pressure. The crude product was purified by column chromatography on silica gel, using hexane/CH_2Cl_2 (1:1) as the eluent, to yield 4.9 g (74%) of **2l**. - ^{1}H NMR: δ = 0.88 (t, 6H, CH_3), 1.25 (m, 54H, CH_2, alkyl chain), 1.86 (m, 4H, CH_2), 2.00 (m, 8H, CH_2), 4.18 (q, 4H, CH_2), 5.35 (m, 4H, CH_2). - ^{13}C NMR: δ = 171.8 (C=O), 129.8 (CH=CH), 129.7 (CH=CH), 60.7 (CH_2O), 57.4 (qC), 32.5, 32.1, 31.8, 29.7, 29.6, 29.4, 29.3, 29.2, 29.0, 27.1, 23.8, 22.6 (CH_2, alkyl chain), 14.0 (CH_3).

2-Alkyl-1,3-propanediols (**3f-l**): Compounds **3a**[31] and **3b**[32] have been described in the literature.

2,2-Didecyl-1,3-propanediol[5h] (**3f**): In a typical experiment, a solution of 8.81 g (0.02 mol) of **2f** in 25 ml of diethyl ether was added to 25 ml of a 1 M solution of $LiAlH_4$ in THF at such a rate that the reaction mixture refluxed gently. Refluxing was continued for 3 h. At 0°C the excess of $LiAlH_4$ was carefully destroyed with ice and a 2 N H_2SO_4 solution, until the solution became clear. The organic layer was separated from the aqueous layer, which was extracted with diethyl ether (3 × 25 ml). The combined organic layers were washed with water and a saturated $NaHCO_3$ solution, dried with Na_2SO_4, and filtered. The solvent was removed under reduced pressure. The crude product (7.0 g, 98%) was crystallized from petroleum ether (boiling range 40-60°C) yielding white, crystalline **3f**. M.p. 30-32°C. - ^{1}H NMR: δ = 0.86 (t, 6H, CH_3), 1.24 (m, 34H, CH_2), 2.03 (t, 4H), 3.55 (d, $J_{H,OH}$ = 4.4 Hz, 4H, CH_2). - ^{13}C NMR: δ = 69.1 (CH_2O), 40.8 (qC), 31.8, 30.6, 30.5, 29.6, 29.3, 22.8, 22.6 (CH_2, alkyl chain), 14.0 (CH_3). - $C_{23}H_{48}O_2$ (356.638): calcd. C 77.46, H 13.57; found C 77.41, H 13.55.

2-Dodecyl-2-methyl-1,3-propanediol[33] (**3g**): M.p. 68-69°C (petroleum ether). - $C_{16}H_{34}O_2$ (258.448): calcd. C 74.36, H 13.26; found C 74.19, H 13.15. - ^{1}H NMR: δ = 0.80 (s, 3H, CH_3), 0.85 (t, 3H, CH_3), 1.25 (m, 20H, CH_2, alkyl chain), 2.45 (s, 2H, CH_2), 3.52 (AB system, 4H, CH_2O). - ^{13}C NMR: δ = 70.6 (CH_2OH), 38.7 (qC), 33.9, 31.8, 30.5, 29.6, 29.3, 23.2, 22.6, 18.4 (CH_2, alkyl chain), 14.0 (CH_3).

2,2-Didodecyl-1,3-propanediol[5h] (**3h**): M.p. 41-43°C (petroleum ether, boiling range 60-80°C). Yield: 87%. - $C_{27}H_{56}O_2$ (412.746): calcd. C 78.57, H 13.68; found C 78.72, H 13.61.

2-Dodecyl-2-hexadecyl-1,3-propanediol (**3i**): M.p. 51-51°C (hexane). Yield: 87%. - $C_{31}H_{64}O_2$ (468.835): calcd. C 79.42, H 13.76; found C 79.32, H 13.50. - ^{1}H NMR: δ = 0.88 (t, 6H, CH_3), 1.26 (m, 52H, CH_2, alkyl chain), 2.25 (br. s, 2H, OH), 3.57 (s, 4H, CH_2OH). - ^{13}C NMR: δ = 69.32 (CH_2OH), 40.92 (qC), 31.79, 30.74, 30.48, 29.57, 29.47, 29.23, 22.74, 22.55 (CH_2, alkyl chain), 13.95 (CH_3).

2,2-Ditetradecyl-1,3-propanediol[5h] (**3j**): M.p. 77-78°C. - ^{1}H-NMR and ^{13}C-NMR spectra are similar to those of **3f** with small differences in the integrals.

2,2-Dihexadecyl-1,3-propanediol[5h] (**3k**): M.p. 83-84°C. - ^{1}H-NMR and ^{13}C-NMR spectra are similar to those of **3f**.

2,2-Bis(cis-9-octadecenyl)-1,3-propanediol (**3l**): Colourless liquid. Purified by column chromatography on silica gel, eluent: CH_2Cl_2 containing 5% of CH_3OH. Yield: 97%. - ^{1}H NMR: δ = 0.89 (t, 6H, CH_3), 1.27 (m, 52H, CH_2 alkyl chain), 2.00 (m, 8H, CH_2), 3.58 (s, 4H, CH_2), 5.36 (m, 4H, CH). - ^{13}C NMR: δ = 129.9 (CH=CH), 129.8 (CH=CH), 69.4 (CH_2O), 40.9 (qC), 32.6, 31.9, 30.7, 30.6, 29.7, 29.6, 29.3, 29.2, 27.2, 22.8, 22.7 (CH_2, alkyl chain), 14.1 (CH_3).

Compounds **4a**, **4b**, **4f-l** were not isolated. Purity and yields as determined by ^{1}H, ^{13}C, and ^{31}P NMR were almost 100%.

2-Chloro-5-decyl-1,3,2-dioxaphosphorinan-2-one (**4a**): To a solution of 1.082 g (0.05 mol) of **3a** in 10 ml of CH_2Cl_2 was added dropwise 0.767 g (0.05 mol) of $POCl_3$ in 1 ml of CH_2Cl_2. The reaction mixture was refluxed for 3.5 h, until the formation of HCl gas had stopped. The solvent was removed under reduced pressure. The residue was a colourless liquid **4a**. - ^{1}H NMR: δ = 0.82 (t, 3H, CH_3), 1.20 (m, 17H, CH_2, alkyl chain), 1.67 (m, 1H, CH), 1.77-2.34 (m, 1H, CH), 2.38-4.58 (m, 4H, CH_2). – ^{31}P NMR: δ = 2.30, -1.75 (ratio 40/60). - ^{13}C NMR: δ = 74.05 (CH_2O, $J_{C,P}$ = 8 Hz), 73.48 (CH_2O, $J_{C,P}$ = 8 Hz), 34.84 (CH, $J_{C,P}$ = 7 Hz), 34.70 (CH_2, $J_{C,P}$ = 7 Hz), 31.7, 29.4, 29.3, 29.2, 29.1, 29.0, 27.6, 26.7, 26.3, 25.9, 22.5 (CH_2, alkyl chain), 13.9 (CH_3).

2-Hydroxy-5-decyl-1,3,2-dioxaphosphorinan-2-one (**5a**): Compound **4a** was dissolved in 100 ml of a 90-% acetone/water solution and refluxed until the hydrolysis was complete (24-28 h). The conversion was monitored by ^{31}P NMR. The solvent was removed under reduced pressure affording white, solid **5a** in 90% yield. M.p. 123-125°C (petroleum ether boiling range 60-80°C). - ^{1}H NMR: δ = 0.88 (t, 3H, CH_3), 1.25 (m, 18H, CH_2, alkyl chain), 2.12 (m, 1H, CH), 4.05-4.42 (m, 4H, CH_2). - ^{31}P NMR: δ = -4.19. - ^{13}C NMR: δ = 72.4 (CH_2O, $J_{C,P}$ = 5.7 Hz), 31.9, 29.6, 29.5, 29.3, 26.7 (CH_2, alkyl chain), 14.1 (CH_3).

2-Chloro-5-dodecyl-1,3,2-dioxaphosphorinan-2-one (**4b**): The NMR spectra were similar to those of **4a**.

5-Dodecyl-2-hydroxy-1,3,2-dioxaphosphorinan-2-one (**5b**): M.p. 125-127°C (petroleum ether, boiling range 60-80°C). Yield: 76%. - $C_{15}H_{31}O_4P$ (306.382): calcd. C 58.80, H 10.20, P 10.11; found C 58.83, H 10.26, P 10.04. The NMR data were similar to those of **5a**.

2-Chloro-5,5-didecyl-1,3,2-dioxaphosphorinan-2-one (**4f**): ^{1}H NMR: δ = 0.88 (t, 6H, CH_3), 1.16 (s, 4H, CH_2), 1.25 (m, 30H, CH_2, alkyl chain), 1.65 (m, 2H, CH_2), 4.07-4.2 (m, 4H, CH_2O).

- ^{31}P NMR: δ = -1.77. - ^{13}C NMR: δ = 76.87 (CH_2O, $J_{C,P}$ = 8 Hz), 37.04 (q, $J_{C,P}$ = 6 Hz), 31.7, 30.5, 30.0, 29.7, 29.6, 29.4, 29.3, 29.1, 29.0, 22.6, 22.5, 22.3 (CH_2, alkyl chain), 13.9 (CH_3).

5,5-Didecyl-2-hydroxy-1,3,2-dioxaphosphorinan-2-one (**5f**): M.p. 70-72°C (methanol). Yield: 98%. - $C_{23}H_{47}O_4P$ (418.599): calcd. C 66.00, H 11.32, P 7.40; found C 66.21, H 11.44, P 7.39. - ^{1}H NMR: δ = 0.88 (t, 6H, CH_3), 1.25 (m, 32H, CH_2, alkyl chain), 1.36 (m, 4H, CH_2), 4.08 (d, $J_{H,P}$ = 12 Hz, 4H, CH_2O), 7.56 (br. s, 1H, OH). – ^{13}P NMR: δ = -3.49. - ^{13}C NMR: δ = 75.34 (CH_2O, $J_{C,P}$ = 6 Hz), 37.0 (qC, $J_{C,P}$ = 6 Hz), 31.7, 30.5, 30.0, 29.7, 29.6, 29.4, 29.3, 19.1, 29.0, 22.6, 22.5, 22.3 (CH_2, alkyl chain), 13.9 (CH_3).

2-Chloro-5-dodecyl-5-methyl-1,3,2-dioxaphosphorinan-2-one (**4g**): ^{1}H NMR: δ = 0.84 (t, 3H, CH_3), 1.23 (m, 21 H, CH_2, alkyl chain), 1.24 (s, 3H, CH_3), 1.64 (br. s, 1H), 3.95-4.28 (m, 4H, CH_2). - ^{31}P NMR: δ = -2.08, -2.34. - ^{13}C NMR: δ = 78.5 ($J_{C,P}$ = 8 Hz), 77.2 (CH_2O, $J_{C,P}$ = 8 Hz), 34.7 (qC, $J_{C,P}$ = 6 Hz), 34.1, 32.8, 31.7, 29.9, 29.7, 29.4, 29.3, 29.1, 23.0, 22.5, 18.9 (CH_2, alkyl chain), 16.7 (CH_3), 13.9 (CH_3).

5-Dodecyl-2-hydroxy-5-methyl-1,3,2-dioxaphosphorinan-2-one (**5g**): M.p. 82-83°C (petroleum ether). Yield: 72%. - ^{1}H NMR: δ = 0.87 (t, 3H, CH_3), 0.98 (t, 3H, CH_3), 1.25 (m, 22H, CH_2, alkyl chain), 4.05 (m, $J_{H,P}$ = 12 Hz, 4H). – ^{31}P NMR: δ = -4.18. - ^{13}C NMR: δ = 76.4 (CH_2O), 34.8 (qC, $J_{C,P}$ = 5 Hz), 33.8, 31.9, 30.1, 29.6, 29.3, 23.1, 22.7 (CH_2, alkyl chain), 18.1 (CH_3), 14.1 (CH_3). - $C_{16}H_{33}O_4P$ (320.409): calcd. C 59.98, H 10.38, P 9.67; found C 60.11, H 10.29, P 9.74.

2-Chloro-5,5-didodecyl-1,3,2-dioxaphosphorinan-2-one (**4h**): Chemical shifts are similar to those of **4f**.

5,5-Didodecyl-2-hydroxy-1,3,2-dioxaphosphorinan-2-one (**5h**): M.p. 74-75°C (methanol). Yield: 88%. - $C_{27}H_{55}O_4P$ (474.707): calcd. C 68.32, H 11.68, P 6.52; found C 68.66, H 11.82, P 6.60. - Chemical shifts are similar to those of **5f**.

2-Chloro-5-dodecyl-5-hexadecyl-1,3,2-dioxaphosphorinan-2-one (**4i**): ^{1}H NMR: δ = 0.91 (t, 6H, CH_3), 1.27 (m, 50H, CH_2, alkyl chain), 1.66 (br. s, 2H, CH_2), 4.06-4.23 (m, 4H, CH_2O). – ^{31}P NMR: δ = -1.75.

5-Dodecyl-5-hexadecyl-2-hydroxy-1,3,2-dioxaphosphorinan-2-one (**5i**): M.p. 71-73°C (acetone). Yield: 65%. - $C_{31}H_{63}O_4P$ (530.816): calcd. C 70.15, H 11.96, P 5.83; found C 70.41, H 11.97, P 5.68. - Chemical shifts are similar to those of **5f**.

2-Chloro-5,5-ditetradecyl-1,3,2-dioxaphosphorinan-2-one (**4j**): Chemical shifts are similar to those of **4f**.

2-Hydroxy-5,5-ditetradecyl-1,3,2-dioxaphosphorinan-2-one (**5j**): M.p. 83-84°C (acetone). Yield: 89%. - $C_{31}H_{63}O_4P$ (530.816): calcd. C 70.15, H 11.96, P 5.83; found C 70.34, H 12.02, P 5.84. - Chemical shifts are similar to those of **5f**.

2-Chloro-5,5-dihexadecyl-1,3,2-dioxaphosphorinan-2-one (**4k**): Chemical shifts are similar to those of **4f**.

5,5-Dihexadecyl-2-hydroxy-1,3,2-dioxaphosphorinan-2-one (**5k**): M.p. 85-86°C (acetone). Yield: 98%. - $C_{35}H_{71}O_4P$ (586.924): calcd. C 71.63, H 12.19, P 5.28; found C 71.69, H 12.31, P 5.27. - Chemical shifts are similar to those of **5f**.

2-Chloro-5,5-di-cis-9-octadecenyl-1,3,2-dioxaphosphorinan-2-one (**4l**): ^{1}H NMR: δ = 0.89 (t, 6H, CH_3), 1.28 (m, 50H, CH_2, alkyl chain), 1.68 (br. s, 2H, CH_2), 2.03 (br. s, 8H, CH_2), 4.2 (m, 4H, CH_2), 5.36 (m, 4H, CH_2). – ^{31}P NMR: δ = -1.72. - ^{13}C NMR: δ = 129.8 (CH), 129.6 (CH), 76.9 (CH_2O), 37.2, 37.1, 32.5, 31.8, 30.7, 30.1, 29.8, 29.7, 29.4, 29.3, 29.2, 29.1, 27.1, 26.5, 22.8, 22.6, 22.4 (CH_2, alkyl chain), 14.0 (CH_3).

2-Hydroxy-5,5-bis(cis-9-octadecenyl)-1,3,2-dioxaphosphorinan-2-one (**5l**): Waxy solid, crystallized from acetone/acetonitrile (1:1). Yield: 93%. - ^{1}H NMR: δ = 0.88 (t, 6H, CH_3), 1.27 (m, 52H, CH_2, alkyl chain), 2.02 (m, 8H, CH_2), 4.08 (d, $J_{H,P}$ = 12.4 Hz, 4H, CH_2), 5.3 (m, 4H, CH). – ^{31}P NMR: δ = -3.41. - ^{13}C NMR: δ = 129.9 (CH), 129.7 (CH), 75.3 (CH_2, $J_{C,P}$ = 5 Hz), 37.1 (qC), 32.5, 31.8, 30.4, 30.1, 29.7, 29.6, 29.5, 29.4, 29.2, 29.1, 29.0, 27.1, 22.7, 22.6 (CH_2, alkyl chain), 14.0 (CH_3). - $C_{39}H_{75}O_4P$ (639.001): calcd. C 73.31, H 11.83, P 4.85; found C 73.17, H 11.86, P 4.76.

Sodium Salts of **5a**, **b**, **f-l** (**6a**, **b**, **f-l**): Compounds **5a**, **b**, **f-l** were dissolved in ethanol. One equivalent of C_2H_5ONa was added (final concentration was about 0.001 mol in 10 ml of ethanol). The reaction mixture was heated until the solution became clear and was left overnight for crystallization. Compound **5l** yielded a waxy solid **6l**.

Scheme 2. Synthetic route to the sodium salts of 5-alkyl-2-hydroxy-1,3,2-dioxaphosphorinan-2-ones and of 5,5-dialkyl-2-hydroxy-1,3,2-dioxaphosphorinan-2-ones

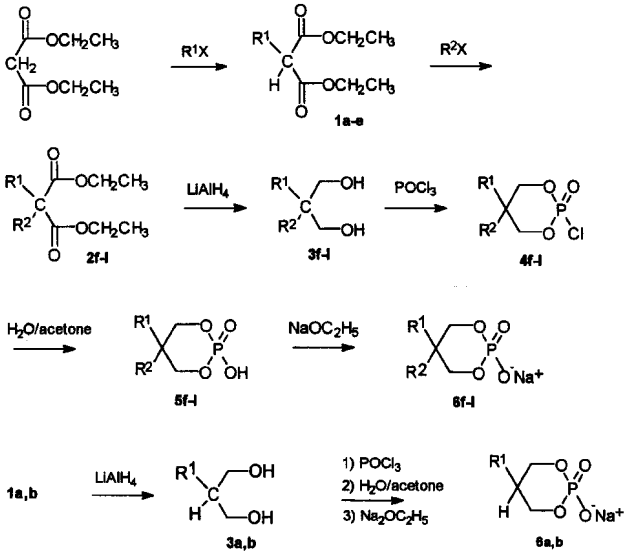

a: $R^1 = C_{10}H_{21}$ **g:** $R^1 = C_{12}H_{25}$, $R^2 = CH_3$
b: $R^1 = C_{12}H_{25}$ **h:** $R^1 = C_{12}H_{25}$, $R^2 = C_{12}H_{25}$
c: $R^1 = C_{14}H_{29}$ **i:** $R^1 = C_{12}H_{25}$, $R^2 = C_{16}H_{33}$
d: $R^1 = C_{16}H_{33}$ **j:** $R^1 = C_{14}H_{29}$, $R^2 = C_{14}H_{29}$
e: $R^1 = C_{18}H_{35}$ **k:** $R^1 = C_{16}H_{33}$, $R^2 = C_{16}H_{33}$
f: $R^1 = C_{10}H_{21}$, $R^2 = C_{10}H_{21}$; **l:** $R^1 = C_{18}H_{35}$, $R^2 = C_{18}H_{35}$

Calcium Salt of **5h**: To 73.9 mg (0.14 mmol) of **5h** in 2 ml of 50% acetic acid was added 14.2 mg (0.07 mmol) of calcium acetate in 1 ml of 50% acetic acid. The white crystalline product was washed with water and dried at 40°C in vacuo (m.p. 212-215°C).

Magnesium Salt of **5h**: To 64 mg (0.116 mmol) of **5h** in 1 ml of 50% acetic acid was added 12.4 mg (0.06 mmol) of magnesium acetate. The white crystalline product was washed with water and dried for 5 hours at 40°C (m.p. 142-148°C).

[1] J. N. Israelachvili, D. J. Mitchell, B. W. Ninham, *J. Chem. Soc., Faraday Trans. 2*, **1976**, *72*, 1525-1568.
[2] J. H. Fendler, *Membrane Mimetic Chemistry*, Wiley-Interscience, New York **1982**.
[3] T. Kunitake, Y. Okahata, *J. Am. Chem. Soc.* **1977**, *99*, 3860-3861.
[4] J. B. F. N. Engberts, D. Hoekstra, *Biochem. Biophys. Acta* **1995**, *1241*, 323-340.
[5] [5a] G.-W. Wang, X-Y. Lei, Y-C. Liu, *J. Am. Oil Chem. Soc.* **1993**, *70*, 731-732. - [5b] G.-W. Wang, X-Y. Yuan, Y-C. Liu, X-G. Lei, *J. Am. Oil Chem. Soc.* **1994**, *71*, 727-730. - [5c] G-W. Wang, X-Y. Yuan, Y-C. Liu, X-G. Lei, Q-X. Guo, *J. Am. Oil Chem. Soc.* **1995**, *72*, 83-87. - [5d] D. Ono, S. Yamamura, M. Nakamura, T. Takeda, A. Masuyama, Y. Nakatsuji, *J. Am. Oil Chem. Soc.* **1995**, *72*, 853-856. - [5e] D. Ono, A. Masuyama, Y. Nakatsuji, M. Okahara, S. Yamamura, T. Takeda, *J. Am. Oil Chem. Soc.* **1993**, *70*, 29-36. - [5f] S. Yamamura, M. Nakamura, T. Takeda, *J. Am. Oil Chem. Soc.* **1989**, *66*, 1165-1170. - [5g] A. Bieniecki, K. A. Wilk, J. Gapinski, *J. Phys. Chem. B* **1997**, *101*, 871-875. - [5h] G.-W. Wang, Y.-C Liu, X.-Y Yuan, X.-G Lei, Q.-X Guo, *J. Coll. Interface Sci* **1995**, *173*, 49-53. - [5i] L. Gan, G. R. Deen, Y. Y. Gan, C. H. Chew, *J. Colloid Interface Sci.* **1996**, *183*, 329-338. - [5j] D. A. Jaeger, E. Kubicz-Loring, R. C. Price, H. Nakagawa, *Langmuir* **1996**, *12*, 5803-5808. - [5k] A. Sokolowski, A. Bieniecki, K. A. Wilk, B. Burczyk, *Colloids Surf. A* **1995**, *98*, 73-82. - [5l] B. R. Bailey, *Surfactant Sci. Ser.* **1990**, *34*, 187-215.
[6] [6a] E. Streefland, A. Wagenaar, D. Hoekstra, J. B. F. N. Engberts, *Langmuir* **1993**, *9*, 219-222. - [6b] L. A. M. Rupert, J. F. L. van Breemen, E. F. J. van Bruggen, J. B. F. N. Engberts, D. Hoekstra, *J. Membr. Biol.* **1987**, *95*, 255-263. - [6c] L. A. M. Rupert, D. Hoekstra, J. B. F. N. Engberts, *J. Colloid Interface Sci.* **1987**, *120*, 125-134. - [6d] L. A. M. Rupert, D. Hoekstra, J. B. F. N. Engberts, *J. Phys. Chem.* **1988**, *92*, 4416-4420. - [6e] L. A. M. Rupert, D. Hoekstra, J. B. F. N. Engberts, *Biochemistry* **1988**, *27*, 8232-8239. - [6f] A. Wagenaar, L. Streefland, D. Hoekstra, J. B. F. N. Engberts, *J. Phys. Org. Chem.* **1992**, *5*, 451-456.
[7] Y. Chevalier, C. Chachaty, *Coll. Polymer Sci.* **1984**, *262*, 489-496.
[8] L. Streefland, F. Yuan, P. Rand, D. Hoekstra, J. B. F. N. Engberts, *Langmuir* **1992**, *8*, 1715-1717.
[9] A. Wagenaar, L. A. M. Rupert, J. B. F. N. Engberts, *J. Org. Chem.* **1989**, *54*, 2638-2642.
[10] M. J. Blandamer, B. Briggs, P. M. Cullis, J. B. F. N. Engberts, A. Wagenaar, E. Smits, D. Hoekstra, A. Kacperska, *J. Chem. Soc., Faraday Trans.* **1994**, *90*, 2709-2715.
[11] M. Shinitzky, Y. Barenholz, *Biochim. Biophys. Acta* **1978**, *515*, 367-394.
[12] B. L. Silver, *The Physical Chemistry of Membranes*, Solomon Press, New York, 1985, p. 241.
[13] T. A. A. Fonteyn, D. Hoekstra, J. B. F. N. Engberts, *J. Am. Chem. Soc.* **1990**, *112*, 8870-8872.
[14] K. Kalyansundaram, J. K. Thomas, *J. Am. Chem. Soc.* **1977**, *99*, 2039-2044.
[15] E. Ralston, L. M. Hjelmeland, R. D. Klausner, J. N. Weinstein, R. Blumenthal, *Biochem. Biophys. Acta* **1981**, *649*, 133-137.
[16] K. Bijma, J. B. F. N. Engberts, G. Haandrikman, N. M. Van Os, M. J. Blandamer, M. D. Butt, P. M. Cullis, *Langmuir* **1994**, *10*, 2578-2582.
[17] M. L. Corrin, H. B. Klevens, W. D. Harkins, *J. Chem. Phys.* **1946**, *14*, 480-486.
[18] J. M. H. Kremer, W. v. d. Esker, C. Pathmamanoharan, P. H. Wiersema, *Biochemistry* **1977**, *16*, 3932-3935.
[19] M. J. Blandamer, B. Briggs, P. M. Burgess, P. M. Cullis, J. A. Green, M. Waters, G. Soldi, J. B. F. N. Engberts, D. Hoekstra, *J. Chem. Soc., Faraday Trans.* **1992**, *85*, 3431-3439.
[20] D. K. Struck, D. Hoekstra, R. E. Pagano, *Biochemistry* **1981**, *20*, 4093-4099.
[21] R. H. Haschemeyer, R. J. Meyers in *Principles and Techniques of Electron Microscopy* (Ed.: M. A. Hayat), Van Nostrand Reinhold, New York, **1972**, volume 2, chapter 3.
[22] J. N. Weinstein, E. Ralston, L. D. Leserman, R. D. Klausnar, P. Dragsten, P. Henkart, R. Blumenthal in *Liposome Technology* (Ed.: G. Gregoriadis), CRC Press, Boca Raton, Florida, **1984**, vol. 3, p. 183.
[23] K. Thomas, G. Weitzel, P. Neumann, *Z. Physiol. Chem.* **1947**, *282*, 192-200.
[24] D. E. Floyd, S. E. Miller, *J. Am. Chem. Soc.* **1947**, *69*, 2354-2355.
[25] L. E. Fieser, E. M. Chamberlin, *J. Am. Chem. Soc.* **1948**, *70*, 71-75.
[26] J. Von Braun, O. Schattner, *Ber. Dtsch. Chem. Ges.* **1941**, *74*, 22-26.
[27] A. Lopez, J. Fidel, C. Alonso Cermeno, *An. Quim.* **1969**, *55*, 153-162 [*Chem. Abstr.* **1969**, *71*, 2923t].
[28] G. Weitzel, J. Wojahn, *Z. Physiol. Chem.* **1950**, *285*, 220-229.
[29] H. Staudinger, G. Bier, G. Lorentz, *Makromol. Chem.* **1949**, *3*, 251-280.
[30] K. E. Schulte, W. Weisskopf, J. Kirschner, *Z. Physiol. Chem.* **1951**, *288*, 69-82.
[31] J. Skarzewski, J. Mochowski, *Tetrahedron* **1983**, *39*, 309-312.
[32] D. E. Ames, R. E. Bowman, *J. Chem. Soc.* **1952**, 1057-1068.
[33] S. Kitazawa, K. Kimura, H. Yano, T. Shono, *J. Am. Chem. Soc.* **1984**, *106*, 6978-6983.

[97071]